J. Med. Plants 2022; 21(81): 22-32

Institute of Medicinal Plants

Journal of Medicinal Plants

Journal homepage: www.jmp.ir

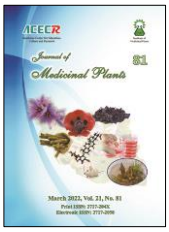

Research Article

Process optimization for green synthesis of iron nanoparticles by extract of fenugreek (*Trigonella foenum-graecum* L.) seeds

Reza Ghafarzadegan[1], Mahdi Yaghoobi[2], Saeideh Momtaz[1], Nasim Ashouri[3], Mona Ghiaci-Yekta[1], Reza Hajiaghaee[1,*]

[1] *Medicinal Plants Research Center, Institute of Medicinal Plants, ACECR, Karaj, Iran*
[2] *Department of Phytochemistry, Medicinal Plants and Drugs Research Institute, Shahid Beheshti University, Tehran, Iran*
[3] *Food and Drug Research Center, Food and Drug Organization, MOH & ME, Tehran, Iran*

ARTICLE INFO

Keywords:
Extract
Fenugreek
Green synthesis
Iron
Nanoparticles
RSM

ABSTRACT

Background: The green synthesis of nanoparticles using plants presents important advantages over other biological systems. Natural compounds present in plant extracts can reduce metal ions to nanoparticles in a single-step green synthesis process. Seeds of fenugreek with various compounds and antioxidant activity are suitable for green synthesis. **Objective:** In this study, the performance of fenugreek seeds extract was evaluated for iron nanoparticles production. **Methods:** The fenugreek (*Trigonella foenum-graecum* L.) seeds were extracted with a distilled water solution at environmental temperature and this aqueous extract was used for the iron nanoparticles synthesis. Response surface methodology was applied to optimize nanoparticle production by considering three independent variables: the extract to metal ion ratio (1.5-6.5), incubation time (30-90 min), and temperature (35-65 °C). **Results:** Mixing the fenugreek seeds extract and iron salt solution with a volume ratio of 1.5 at 36.5 °C for 90 min led to the optimization of iron nanoparticle production with the narrowest size distribution. At the optimized condition, the nanoparticle size was in the range of 20-40 nm. **Conclusion:** Iron nanoparticles were successfully synthesized with fenugreek seed extract. Physical parameters such as time, temperature, and mixing volume ratio of the extract to metal ions can control the average size of the synthesized green iron nanoparticles.

1. Introduction

The appearance of nanotechnology in the 1960s started a new era of materials science [1]. This appears as the sixth revolutionary technology after the other five revolution, i.e., industrial, nuclear energy, green, information technology, and biotechnology in the past century [2]. Many recent studies have shown

Abbreviations: CCD, Central Composite Design; DPPH, 2,2-Diphenyl-1-Picrylhydrazyl; FTIR, Fourier-Transform Infrared Spectroscopy; INPs, Iron Nanoparticles; RSM, Response Surface Methodology; SEM, Scanning Electron Microscopy; TEM, Transmission Electron Microscopy

*Corresponding author: hajiaghaee@imp.ac.ir

doi: 10.52547/jmp.21.81.22
Received 28 September 2021; Received in revised form 30 December 2021; Accepted 1 January 2022

nanoparticles' potential for their applications in sensors, catalysts, magnetic recording and electronic devices, biomedicine, and removal of pollutants [3].

Several fabrication processes for producing iron nanoparticles (INPs), including chemical and mechanical techniques [4]. Chemical synthesis methods include using toxic chemicals, forming dangerous byproducts, and pollution from precursor chemicals [5]. Therefore, more environmentally friendly and economically feasible techniques are required for nanoparticle synthesis.

In recent years, it has been shown that many biological systems, including plants [6] and algae [7], diatoms [8], bacteria [9], yeast [10], fungi [11], and human cells [12], appeared as green alternatives of synthesis of nanoparticles. The green synthesis of particles using plants presents important advantages over other biological systems, such as the low expense of cultivation, the ability to up output volumes, and it is simpler, safer, and quicker. In the literature, the INPs synthesis has been made using various plants such as *Mentha piperita* [13], *Citrus maxima* [14], *Mentha longifolia* [15], and *Salvia officinalis* [16].

Fenugreek (*Trigonella foenum-graecum* L.) is an annual herb that belongs to the family Leguminosae widely grown in Middle Eastern countries [17]. Both leaves and seeds should be contained in the family's regular diet, especially the diet of growing kids, pregnant ladies, maturity reaching girls, and older family members because they have haematinic (i.e. blood formation) value [18]. The seeds contain the alkaloid trigonelline along with mucilage, tannic acid, yellow coloring matter, fixed and volatile oils, a bitter extractive, diosgenin, gitogenin, a trace of trigogenin, and vitamin A [19]. The seeds are also rich in protein and contain a unique major free amino acid 4-hydroxy isoleucine, characterized as one of the active ingredients in fenugreek seeds [20].

In this study, the performance of fenugreek seed extract was evaluated for INP production. Response surface methodology (RSM) optimized nanoparticle production by considering three independent variables: the incubation time, temperature, and extract: metal ion ratio. Scanning electron microscopy (SEM) was used to investigate the influence of these three variables on nanoparticle size as response variables under 15 designed run experiments. The synthesized nanoparticles at the optimal condition (that verified by SEM) were further analyzed using transmission electron microscopy (TEM) and Fourier-transform infrared spectroscopy (FTIR).

2. Materials and Methods

2.1. Materials

The required materials used in this study are listed as follows: Merck has manufactured ethanol, methanol, ferric chloride ($FeCl_3$), n-hexane, chloroform, dimethyl sulphoxide (DMSO), calcium chloride ($CaCl_2$), Folin-Ciocalteu reagent, hydrochloric acid (HCl), magnesium chloride ($MgCl_2$), potassium chloride (KCl), sodium carbonate (Na_2CO_3), sulphuric acid (H_2SO_4), potassium ferricyanide ($C_6N_6FeK_3$); all these analytical-grade compounds. The following chemicals manufactured by Sigma-Aldrich have also been used: linoleic acid ($C_{18}H_{32}O_2$), 2,2-diphenyl-1-picrylhydrazyl (DPPH), rutin (≥ 94 %). Finally, gallic acid (≥ 98 %) was obtained from Merck.

2.2. Preparation of plant extracts for phytochemical screening and INP formation

The fenugreek seeds were provided by the Institute of Medicinal Plants, ACECR, Karaj,

[DOR: 20.1001.1.2717204.2022.21.81.4.0]
[DOI: 10.52547/jmp.21.81.22]

Iran (code number: 355Tf018MPSB). These were dried, powdered (30 g), packed in a percolator and macerated with a distilled water solution at environmental temperature for three days with three solution changes (210 ml). The extract obtained was filtered using a Whatman filter paper No. 1 and then centrifuged at 6000 rpm for 10 min. This aqueous extract was used for phytochemical screening and INP formation.

2.3. Determination of total phenolic content of plant extract

The total phenolic contents were determined by the Folin-Ciocalteu colorimetric method following a modification of the procedure described by Obanda [21]. In this method, the plant dried extract solution was diluted with 5 ml distilled water mixed with 500 µl of the Folin-Ciocalteu reagent in a volumetric flask. 1 ml of 15 % sodium carbonate solution was added to the mixture and allowed to stand for 30 Min. Then, the absorbance was determined at 725 nm using a spectrophotometer (Human, USA). Gallic acid was used as a standard to produce the calibration curve. The total phenolic content was expressed as mg of gallic acid equivalents per dried extract (g). All samples were analyzed in triplicates.

2.4. Determination of total flavonoid assay

Total flavonoid content was estimated by aluminum chloride colorimetric assay. An aliquot (1 ml) of extracts and a standard solution of rutin (250, 500, 750, 1000 and 1250 mg/L) was added to a 10 ml volumetric flask containing 4 ml of distilled deionized water (dd H_2O). After 5 min, 0.3 ml 10 % $AlCl_3$ was added, and the total volume was made up to 10 ml with dd H_2O. The solution was mixed well, and the absorbance was calculated against the prepared reagent blank at 420 nm with a UV-VIS Spectrophotometer. The total flavonoid contents of the dry extract are expressed as mg of rutin equivalents (RE) per g dry extract (mg RE/1g de). All samples were analyzed in triplicates [22].

2.5. Determination of the antioxidant activity of plant extract using a DPPH assay

The DPPH test was used to estimate the antioxidant capacity of the plant extract [23]. 1 ml of various concentrations (250, 125, 62.5, 31.25, 15.62 and 7.81 µg/ml) of the extract in ethanol was added to 4 ml of 0.004 % methanol solution of DPPH. After a 60 min incubation stage at room temperature, the absorbance was read against a blank at 517 nm. Inhibition of free radical by DPPH in percent (I %) was calculated in the following way:

$$\boldsymbol{I\%} = \left[\frac{\boldsymbol{A\ blank - A\ sample}}{\boldsymbol{A\ blank}}\right] * \mathbf{100}$$

A blank =Absorbance of the control reaction (containing all reagents except the test compound).

A sample = Absorbance of the test compound.

Extract concentration providing 50 % inhibition (IC_{50} %) was calculated from the graph plotted inhibition percentage against extract concentration. IC_{50} % values were compared to IC_{50} % value of a "standard" antioxidant, in this case, ascorbic acid (AA), obtained by the same procedure.

2.6. Green synthesis of INPs

Ferric chloride hexahydrate ($FeCl_3.6H_2O$) was employed as a precursor for nanoparticle synthesis. INPs were synthesized by adding the prepared extract to 0.01 M of $FeCl_3.6H_2O$ under the different operational conditions referred to in Table 1. After the reaction completion, the synthesized nanoparticles were gathered using centrifugation at 6000 rpm for 10 min, followed by repeated washings using double distilled

[DOR: 20.1001.1.2717204.2022.21.81.4.0]
[DOI: 10.52547/jmp.21.81.22]

water and ethanol, respectively. Then the concentrated nanoparticles were dried in a vacuum oven for 24 h and then preserved in a desiccator to inhibit the side effects of oxygen or moisture on the synthesized nanoparticles.

Table 1. The central composite experimental design (in the coded level of three variables) employed for RSM and the average size of the nanoparticles synthesized using fenugreek seeds extract

Run experiments	*X*1 (time)	*X*2 (temperature)	*X*3 (mixing volume ratio)	Average size (nm)
1	60	65	1.5	80.3
2	90	65	4	90.0
3	60	50	4	65.2
4	90	35	4	39.9
5	60	65	6.5	99.9
6	30	50	6.5	73.2
7	30	35	4	100.3
8	90	50	1.5	40.6
9	60	35	6.5	62.6
10	60	35	1.5	55.5
11	90	50	6.5	48.1
12	30	50	1.5	52.0
13	60	50	4	53.3
14	60	50	4	58.2
15	30	65	4	53.9

2.7. Design of experimental conditions

RSM was used in designing this experiment. According to central composite design (CCD) in the response surface method, a set of 15 experimental trials, was generated using the statistical software MINITAB version 16.0 (Table 1). Three factors [X1 (time), X2 (temperature), and X3 (mixing volume ratio)], at three levels, were considered. The experimental procedure consists of 15 runs, and the independent variables are studied at three levels: low (−1), medium (0), and high (+1) (Table 2). To correlate the average size of the nanoparticles with the operational parameters, the quadratic polynomial model, as shown below, can be helpful:

$$Y = \beta_0 + \sum_{i=1}^{4} \beta_i X_i + \sum_{i=1}^{4} \beta_{ii} X_i^2 + \sum_{i=1}^{4} \sum_{j>1}^{4} \beta_{ij} X_i X_j$$

Where Y characterizes the predicted response variable, β_0 is the model intercept; β_i, β_{ii}, and β_{ij} are the regression coefficients of linear, square, and interaction terms, respectively. X_i and X_j show the coded independent variables. The second-order polynomial coefficients were calculated and analyzed using the MINITAB statistical software (version 16.0). The data obtained from CCD was assessed using regression analysis and analysis of variance (ANOVA).

2.8. UV-Vis spectroscopy of INPs

The synthesizing of samples was monitored at various intervals, diluted with distilled water 100 folds, and then their absorbance was measured by a UV-Vis spectrophotometer (X-ma 2000, Varian, Human Corporation, USA) a resolution of 1 nm in the range of 200-900 nm.

Table 2. Selected factors and their coded levels

Symbols	Factors	Coded levels		
		-1	0	+1
X_1	Time (min)	30	60	90
X_2	Temperature (°C)	35	50	65
X_3	Mixing volume ratio (v/v)	1.5	4	6.5

2.9. Scanning electron microscopy of INPs

The morphological evaluation of the synthesized Fe nanoparticles was conducted on SEM (EM3200, KYKY, and China), operating at 26 kV with a magnification of × 40,000. For the SEM analysis, the purified synthesized INPs were located on the SEM holder and then gold-coated using sputter coated.

2.10. Transmission electron microscopy of INPs

The morphological analysis of the produced nanoparticles was operated using a transmission electron microscope (EM10C-100 KV, Zeiss, Germany) operating at 100 kV. TEM samples were prepared using the drop-casting of the colloidal INPs on the carbon-coated copper grids and were allowed to dry at room temperature.

2.11. Fourier-transform infrared spectroscopy of INPs

To achieve a deeper insight into the mechanism of INP formation, the presence of functional groups on the surface of nanoparticles was investigated by FTIR (Magna-IR™ Spectrometer 550, Nicolet, USA). For sample preparation, the purified nanoparticles were mixed with KBr powder and pressed into a pellet. The FTIR spectra were recorded in the 500-4000 cm^{-1} range with a resolution of 4 cm^{-1}.

3. Results

In this study, the extract of fenugreek seeds was provided by macerating 30g of that and evaporating under a vacuum to reach a dried powder extract. The yield of extraction was 12.26 (%w/w).

3.1. Optimisation of the INP formation by CCD

The three operational parameters (incubation time, temperature, and mixing volume ratio of extract and precursor) were optimized in the present CCD design with a total of 15 runs in Table 1. The average size of the nanoparticles in each experiment was obtained from the corresponding SEM image using the ImageJ software. Table 1 describes the average size of the nanoparticles for the 15 runs listed.

3.2. Characterisation of the synthesized INPs under the optimal conditions

3.2.1. UV-Vis spectroscopy

The Colour change of the reaction mixture containing fenugreek seeds extract and iron salt to dark brownish is the preliminary evidence of INP formation. The development of nanoparticle formation in the reaction solution was studied by UV-Vis spectroscopy. The UV-Vis spectrum of the solution after the end of the reaction is presented in Fig. 1. As shown in this figure, two absorption peaks can be observed at 219 and 269 nm wavelengths. The development of INPs occurs via the subsequent steps: (1) complexation with Fe salts, (2) simultaneous reduction of Fe (II) capping with oxidized polyphenols. The absorption peaks at 219 nm are identical to the characteristic UV visible spectrum of metallic iron [24]. The absorption peak at 269 nm shows the interaction between $FeCl_3$ solution and extract of Fenugreek seeds [25-26].

[DOR: 20.1001.1.2717204.2022.21.81.4.0]
[DOI: 10.52547/jmp.21.81.22]

3.2.2. TEM analysis

The morphology and structure of the INPs at higher resolution are shown in the TEM images (Fig. 2a). The particle sizes range from 20 to 40 nm, which is consistent with the size distribution obtained from the SEM analysis. It can be seen that the produced nanoparticles have an experimental shape. Moreover, the TEM micrograph (Fig. 2b) shows some degrees of agglomerations due to the high surface energy of the nanoparticles.

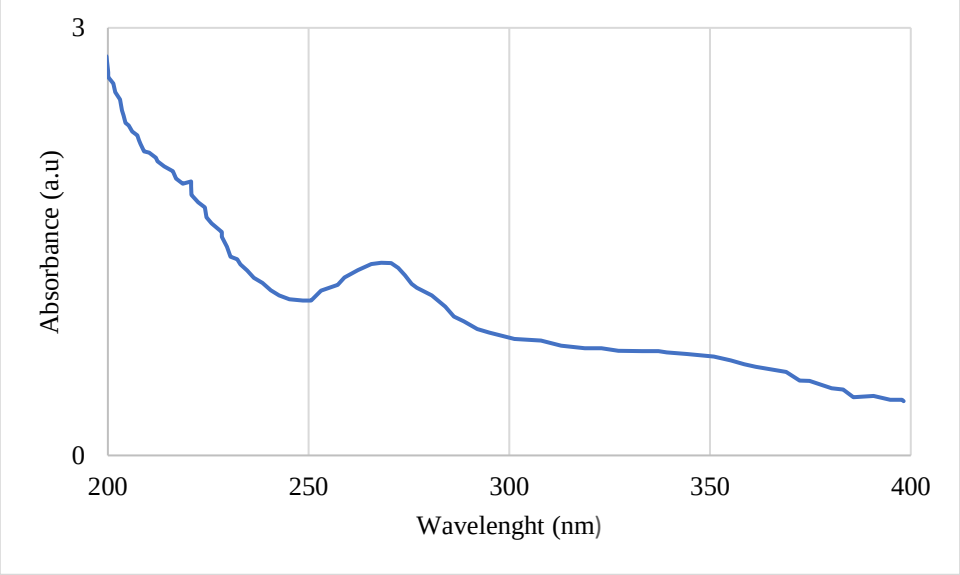

Fig. 1. UV–Vis spectrum of the colloidal solution of INPs in reaction mixtures containing fenugreek seeds extract and iron salt with the volume ratio of 1.5 under 36.5 °C after 90 min

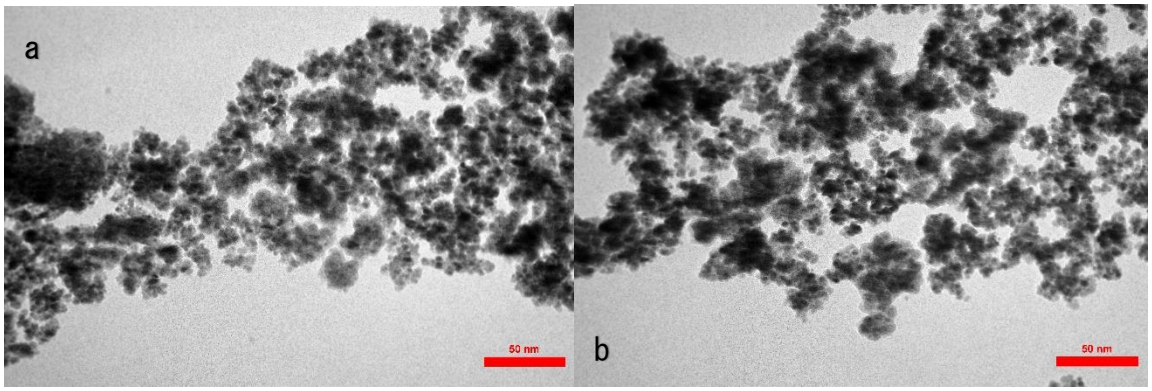

Fig. 2. TEM image of the colloidal INPs synthesized using fenugreek seeds extract in the optimal condition (extract to iron salt volume ratio of 1.5, incubation time of 90 min, and temperature of 36.5 °C)

3.3. Mechanism study of INP formation

3.3.1. Identification of phytochemicals

Test results verify that flavonoid, phenolic content, and antioxidant activity were present in the fenugreek seeds extract. The total phenolic contents were determined by the Folin-Ciocalteu colorimetric method. The total phenolic content of the extract was 1.02 ± 0.03 mg of gallic acid per dried extract (g). Total flavonoid content was estimated by aluminum chloride colorimetric assay. The total flavonoid content of the dry extract was 2.77 ± 0.66 mg of RE per g dry

extract. The DPPH test was used to estimate the antioxidant capacity of the plant seed extract. The IC_{50} % value of that was 3.7 ± 0.003 mg per ml. These compounds with significant antioxidant activity have a key role in reducing the Fe^{3+} ions followed by forming and capping the Fe nanoparticles.

3.3.2. FTIR analysis

FTIR was used to identify the possible natural products in the plant extract responsible for reducing the Fe ions and acting as capping agents. FTIR spectra of the aqueous extract of fenugreek before and the synthesized INPs are presented in Fig. 3.

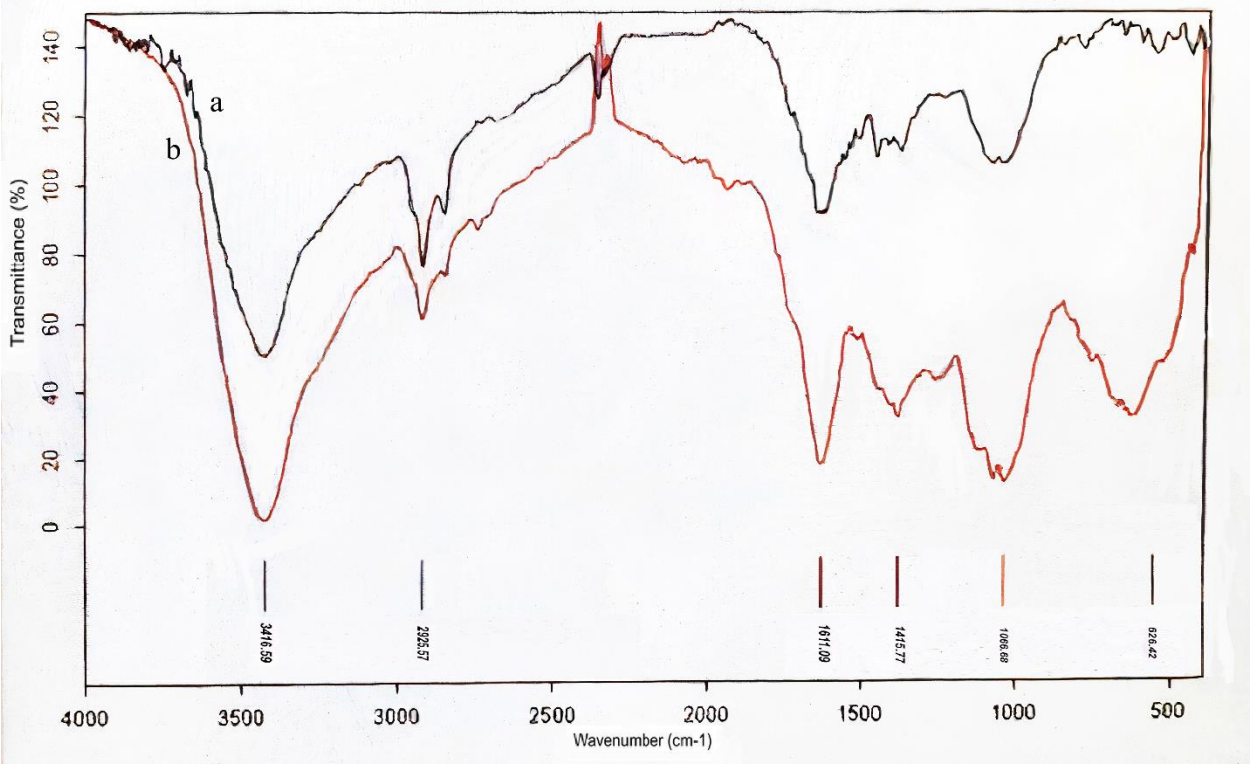

Fig. 3. FTIR spectra of the seeds extract of fenugreek **(a)** After synthesis of INP at the optimal condition **(b)** Before adding Fe^{3+} cations

4. Discussion

From the CCD runs, it was found that the quadratic polynomial model shows the best fit and is expressed as follows:

$$Y = 365.6 - 2.146X_1 - 10.34X_2 + 2.3X_3 + 0.00517X_1^2 + 0.0731X_2^2 - 0.123X_3^2 + 0.054X_1X_2 - 0.0459X_1X_3 + 0.084X_2X_3$$

The ANOVA for the above predicted quadratic model was conducted, and the results are summarized in Table 3. As shown in the table, the model's high F-value of 5.18 and low P-value ($P < 0.05$) prove that the predicted model is statistically significant. Also, 'lack of fit' with *F*-value of 4.30 and a P-value of 0.194 suggests that it is not significant. Non-significant 'lack of fit' indicates the accuracy of the model. The coefficient of determination (R^2) is another criterion for checking the fitness of the model. Higher R^2 values (close to 1) indicate a better correlation between the experimental and the predicted results. R^2 of this model was evaluated as 0.9031, revealing the relatively good correlation between the experimental data and the predicted values by the model.

It is believed that P-value < 0.05 provides insights into the significance of the model terms in (3). As indicated in Table 3, all the linear terms (X_1, X_2, X_3) show non-significant effects, the quadratic terms of temperature (X_1^2, P < 0.05), and the interaction term time × temperature ($X_1 \times X_2$, P < 0.05) show noticeable effects on the average nanoparticle size. Contrarily, two quadratic terms (X_2^2, X_3^2) and the interaction terms (X_1X_3, X_2X_3) show non-significant effects. The model terms with higher F-value and lower P-value tend to be more effective on the response variable. Among all significant terms, F-value of the interaction terms (F-value of 7.69) It is higher than the linear term, indicating the more significant interaction terms of time and temperature on the response variable (Table 3).

Optimum values using MINITAB software were predicted as the temperature of 36.5 °C and mixing volume ratio of 1.5. The corresponding time for these optimum values was 90 min. The minimum average size of the INPs under predicted optimum conditions was calculated as 29.50 nm.

Table 3. Results of ANOVA for response surface model

Source	Degrees of freedom	The adjusted sum of squares	Adjusted mean squares	F-value	P-value
Model	9	4947.47	549.72	5.18	0.042
Linear	3	1357.55	452.52	4.26	0.076
X_1	1	531.38	531.38	5.00	0.076
X_2	1	442.38	442.38	4.16	0.097
X_3	1	383.78	383.78	3.61	0.116
Square	3	1138.57	379.52	3.57	0.102
X_1^2	1	998.95	998.95	9.40	0.028
X_2^2	1	79.81	79.81	0.75	0.426
X_3^2	1	2.18	2.18	0.02	0.892
Interaction	3	2451.35	817.12	7.69	0.025
$X_1 \times X_2$	1	2364.39	2364.39	22.26	0.005
$X_1 \times X_3$	1	39.63	39.63	0.37	0.568
$X_2 \times X_3$	1	47.33	47.33	0.45	0.534
Error	5	531.08	106.22		
Lack-of-Fit	3	459.83	153.28	4.30	0.194
Pure Error	2	71.25	35.62		
Total	14	5478.55			
R^2	0.9031				
R^2-adjusted	0.7286				

The spectra of fenugreek extract in Fig. 3 (b) show the absorption bands at around 1072, 1267, 1411, 1627, 2925, and 3416 cm^{-1}. The band at 1072 cm^{-1} can be related to the C–N stretching vibration of aliphatic amines [27]. The band at 1411 cm^{-1} can be assigned to C = O stretching vibration, which might arise from the functional groups of ketones, aldehydes, and carboxylic acids. The bands observed at 1627 cm^{-1} can be attributed to the C = C stretching vibrations of the aromatic ring, which belongs to the phenol compounds (e.g. flavonoids and polyphenols) [28]. The absorption band associated with the C-H and stretching vibration of aliphatic

hydrocarbon chains appears at 2925 cm^{-1} [25, 28]. The broad bands around 3416 represent the phenolic compounds' O-H stretching, indicating strong hydrogen bonding [30]. These functional groups prove the presence of phenols, aliphatic amines, and organic acids in the extracts, which might reduce and stabilizing agents in the INP synthesis. The FTIR spectra reveal that the observed bands for functionalized INPs (Fig. 3a) are similar to those obtained for fenugreek extract (Fig. 3b) with a slight shift. As far as the IR spectrum is concerned, there is no considerable change in the molecular bonds of functional groups from the extract compounds. The appearance of the absorption band around 450 cm-1 in the FTIR spectrum of INPs (Fig. 3a) is attributable to the small quantities of Fe-O from dissolving Fe_3O_4 and Fe_2O_3. This can be related to the formation of INPs that is partially oxidized due to exposure to air or water 26. The Fe-O stretching vibration band of the bulk magnetite usually appears at 570 cm^{-1}, and the band shifts to the higher wavenumbers (582.82 cm^{-1}, Fig. 3a) because of the finite size of the nanoparticles production [13, 30].

5. Conclusion

We successfully synthesized INPs with the seeds extract of fenugreek. The physical parameters such as time, temperature, and mixing volume ratio of the extract to the metal ions could control the average size of the green synthesized INPs. Transmission electron microscopy (TEM), and Fourier-transform infrared spectroscopy (FTIR) were used for analyzing the synthesized nanoparticles at the optimal condition. Also, we evaluated the cytotoxicity effect of INPs on non-cancerous NIH3T3 cells. MTT results demonstrated that INPs showed no cytotoxicity towards NIH3T3 cells at concentrations tested in this study.

Author contributions

Substantial contributions to design, analysis and interpretation of data: R. G., N. A., M. Y., and R. H.; investigation: S. M., M. G.-Y.; drafting the article or revising: M. Y., N. A., and R. H.; final approval of the version to be published: R. G., and R. H.

Conflicts of interest

The authors confirm that there are no conflicts of interest.

Acknowledgments

This work was supported by grant no. 971304 from National Institute for Medical Research Development.

References

1. VK S, RA Y and Y L. Silver nanoparticles: green synthesis and their antimicrobial activities. *Adv. Colloid Interface Sci*. 2009; 145(1-2): 83-96. doi: 10.1016/J.CIS.2008.09.002.

2. Jeong E, Jung G and Hong CA. research HL-A of pharmacal and 2014 undefined. Gold nanoparticle (AuNP)-based drug delivery and molecular imaging for biomedical applications. *Springer*. 2013; 37(1): 53-59. doi: 10.1007/ s12272-013-0273-5.

3. Xiao Z, Yuan M, Yang B, Liu Z, Huang J and Sun D. Plant-mediated synthesis of highly active iron nanoparticles for Cr (VI) removal: Investigation of the leading biomolecules. *Chemosphere*. 2016; 150: 357-364. doi: 10.1016/j.chemosphere.2016.02.056.

4. Dale LH and Huber D. Synthesis, properties, and applications of iron nanoparticles. *Small*. 2005; 1(5): 482-501. doi: 10.1002/ smll. 200500006.

5. Roy K and Ghosh CK. Biological synthesis of metallic nanoparticles: A green alternative. In: *Nanotechnology: Synthesis to Applications* 2017. doi: 10.1201/9781315116730

6. Ganguly S, Mondal S, Das P, Bhawal P, Das T kanti, Bose M, Choudhary S, Gangopadhyay S, Das AK and Das NC. Natural saponin stabilized nano-catalyst as efficient dye-degradation catalyst. *Nano-Structures and Nano-Objects* 2018; 16: 86-95. doi: 10.1016/j.nanoso. 2018.05.002.

7. Rajeshkumar S, Kannan C and Annadurai G. Green synthesis of silver nanoparticles using marine brown Algae turbinaria conoides and its antibacterial activity. *Int. J. Pharma. Bio. Sci*. 2012; 3(4): 502-510.

8. Chetia L, Kalita D and Ahmed GA. Synthesis of Ag nanoparticles using diatom cells for ammonia sensing. *Sens. Bio-Sensing Res*. 2017; 16: 55-61. doi: 10.1016/j.sbsr.2017.11.004.

9. Mukherjee S and Nethi SK. Biological synthesis of nanoparticles using bacteria. In: *Nanotechnology for Agriculture: Advances for Sustainable Agriculture*. 2019. doi: 10.1007/978-981-32-9370-0_3.

10. Niknejad F, Nabili M, Daie Ghazvini R and Moazeni M. Green synthesis of silver nanoparticles: Another honor for the yeast model Saccharomyces cerevisiae. *Curr. Med. Mycol*. 2015; 1(3): 17-24. doi: 10.18869/ acadpub.cmm. 1.3.17.

11. Sastry M, Ahmad A, Islam Khan M and Kumar R. Biosynthesis of metal nanoparticles using fungi and actinomycete. *Curr. Sci*. 2003; 85(2): 162-170.

12. El-Said WA, Cho HY, Yea CH and Choi JW. Synthesis of metal nanoparticles inside living human cells based on the intracellular formation process. *Adv. Mater*. 2014; 26(6): 910-918. doi: 10.1002/ADMA.201303699.

13. Akhbari M, Hajiaghaee R, Ghafarzadegan R, Hamedi S and Yaghoobi M. Process optimisation for green synthesis of zero-valent iron nanoparticles using Mentha piperita. *IET Nanobiotechnol*. 2019; 13(2): 160-169. doi: 10.1049/iet-nbt.2018.5040

14. Wei Y, Fang Z, Zheng L, Tan L and Tsang EP. Green synthesis of Fe nanoparticles using Citrus maxima peels aqueous extracts. *Mater. Lett*. 2016; 185: 384-386. doi: 10.1016/ j.matlet.2016.09.029.

15. Tavosi F, Ghafarzadegan R, Mirshokraei SA and Hajiaghaee R. Green synthesis of iron nano particles using *Mentha longifolia* L. extract. *J. Med. Plants*. 2018; 17(66): 135-144.

16. Wang Z, Fang C and Mallavarapu M. Characterization of iron-polyphenol complex nanoparticles synthesized by Sage (*Salvia officinalis*) leaves. *Env. Tech. Inno*. 2015; 4: 92-97. doi: 10.1016/j.eti.2015.05.004.

17. Alarcon-Aguilara FJ, Roman-Ramos R, Perez-Gutierrez S, Aguilar-Contreras A, Contreras-Weber CC and Flores-Saenz JL. Study of the anti-hyperglycemic effect of plants used as antidiabetics. *J. Ethnopharmacol*. 1998; 61(2): 101-110. doi: 10.1016/S0378-8741(98)00020-8.

18. Ody P. The Herbs Society's Complete Medicinal Herbal. 1993.

19. Petit PR, Sauvaire YD, Hillaire-Buys DM, Leconte OM, Baissac YG, Ponsin GR and Ribes GR. Steroid saponins from fenugreek seeds: Extraction, purification, and pharmacological investigation on feeding behavior and plasma cholesterol. *Steroids*. 1995; 60(10): 674-680. doi: 10.1016/0039-128X(95)00090-D.

20. Broca C, Gross R, Petit P, Sauvaire Y, Manteghetti M, Tournier M, Masiello P, Gomis R and Ribes G. 4-hydroxyisoleucine: Experimental evidence of its insulinotropic and antidiabetic properties. *Am. J. Physiol-*

Endocrinol Metab. 1999; 2*77*(4): E617-E623. doi:10.1152/AJPENDO.1999.277.4.E617.

21. Obanda M, Owuor PO and Taylor SJ. Flavanol composition and caffeine content of green leaf as quality potential indicators of Kenyan black teas. *J. Sci. Food Agric*. 1997; 74(2): 209-215. doi: 10.1002/(SICI)1097-0010(199706)74:2<209: AID-JSFA789> 3.0. CO; 2-4.

22. Marinova D, Ribarova F and Atanassova M. total phenolics and total flavonoids in bulgarian fruits and vegetables. *Academia. Edu*. 2005; 40(3): 255-260.

23. Yuan YV, Bone DE and Carrington MF. Antioxidant activity of dulse (Palmaria palmata) extract evaluated in vitro. *Food Chem*. 2005; 91(3): 485-494. doi: 10.1016/ j.foodchem. 2004.04.039.

24. Poguberović SS, Krčmar DM, Maletić SP, Kónya Z, Pilipović DDT, Kerkez D V and Rončević SD. Removal of As (III) and Cr (VI) from aqueous solutions using "green" zero-valent iron nanoparticles produced by oak, mulberry and cherry leaf extracts. *Ecol. Eng*. 2016; 90: 42-49.

25. Devatha CP, Thalla AK and Katte SY. Green synthesis of iron nanoparticles using different leaf extracts for treatment of domestic waste water. *J. Clean Prod*. 2016; 139: 1425-1435. doi: 10.1016/j.jclepro.2016.09.019.

Katata-Seru L, Moremedi T, Aremu OS and Bahadur I. Green synthesis of iron nanoparticles using Moringa oleifera extracts and their applications: removal of nitrate from water and antibacterial activity against Escherichia coli. *J. Mol. Liq*. 2018; 256: 296-304.

27. Wang T, Lin J, Chen Z, Megharaj M and Naidu R. Green synthesized iron nanoparticles by green tea and eucalyptus leaves extracts used for removal of nitrate in aqueous solution. *J. Clean Prod*. 2014; 83: 413-419. doi: 10.1016/j. jclepro.2014.07.006.

28. Zhuang Z, Huang L, Wang F and Chen Z. Effects of cyclodextrin on the morphology and reactivity of iron-based nanoparticles using Eucalyptus leaf extract. *Ind. Crops Prod*. 2015; 69: 308-313. doi: 10.1016/ j.indcrop.2015. 02.027.

29. Wang T, Jin X, Chen Z, Megharaj M and Naidu R. Green synthesis of Fe nanoparticles using eucalyptus leaf extracts for treatment of eutrophic wastewater. *Sci. Total Environ*. 2014; 466: 210-213. doi: 10.1016/ j.scitotenv.2013. 07.022.

30. Weng X, Jin X, Lin J, Naidu R and Chen Z. Removal of mixed contaminants Cr(VI) and Cu(II) by green synthesized iron based nanoparticles. *Ecol. Eng*. 2016; 97: 32-39. doi: 10.1016/j.ecoleng.2016.08.003.

How to cite this article: Ghafarzadegan R, Yaghoobi M, Momtaz S, Ashouri N, Ghiaci-Yekta M, Hajiaghaee R. Process optimization for green synthesis of iron nanoparticles by extract of fenugreek **(*Trigonella foenum-graecum* L.) seeds**. ***Journal of Medicinal Plants*** 2022; 21(81): 22-32.
doi: 10.52547/jmp.21.81.22

فصلنامه گیاهان دارویی ۱۴۰۰؛۲۱(۸۱): ۲۲-۳۲

فصلنامه گیاهان دارویی

Journal homepage: www.jmp.ir

پژوهشکده گیاهان دارویی
جهاد دانشگاهی

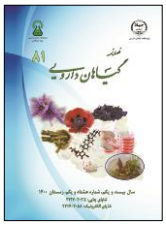

مقاله تحقیقاتی

بهینه‌سازی فرآیند سنتز سبز نانوذرات آهن با استفاده از عصاره دانه شنبلیله

رضا غفارزادگان[۱]، مهدی یعقوبی[۲]، سعیده ممتاز[۱]، نسیم آشوری[۳]، مونا غیاثی یکتا[۱]، رضا حاجی‌آقایی[۱،*]

[۱] مرکز تحقیقات گیاهان دارویی، پژوهشکده گیاهان دارویی جهاد دانشگاهی، کرج، ایران

[۲] گروه فیتوشیمی، پژوهشکده گیاهان و مواد اولیه دارویی، دانشگاه شهید بهشتی، تهران، ایران

[۳] مرکز تحقیقات آزمایشگاهی کنترل غذا و دارو، تهران، ایران

اطلاعات مقاله

گل‌واژگان:
عصاره
شنبلیله
سنتز سبز
آهن
نانوذرات
روش سطح پاسخ

چکیده

مقدمه: سنتز سبز نانوذرات با استفاده از گیاهان مزایای مهمی نسبت به سایر سیستم‌های بیولوژیکی دارد. ترکیبات طبیعی موجود در عصاره‌های گیاهی می‌توانند یون‌های فلزی را در یک فرآیند تک مرحله‌ای به نانوذرات تبدیل کنند. دانه شنبلیله با ترکیبات مختلف و فعالیت آنتی‌اکسیدانی برای این فرآیند مناسب است. **هدف:** در این مطالعه، عملکرد عصاره دانه شنبلیله برای تولید نانوذرات آهن مورد ارزیابی قرار گرفت. **روش بررسی:** عصاره دانه شنبلیله با حلال آب مقطر در دمای محیط استخراج شد و از این عصاره آبی برای سنتز نانوذرات آهن استفاده شد. روش سطح پاسخ برای بهینه‌سازی تولید نانوذرات با در نظر گرفتن سه متغیر مستقل از جمله نسبت عصاره به یون فلزی (۱/۵ تا ۶/۵)، مدت زمان واکنش (۳۰ تا ۹۰ دقیقه) و دما (۳۵ تا ۶۵ درجه سانتی‌گراد) بکار برده شد. **نتایج:** مخلوط کردن عصاره دانه شنبلیله و محلول نمک آهن با نسبت حجم ۱/۵ در دمای ۳۶/۵ درجه سانتی‌گراد به مدت ۹۰ دقیقه منجر به بهینه‌سازی تولید نانوذرات آهن با باریک‌ترین توزیع شد. در شرایط بهینه، اندازه نانوذرات در محدوده ۲۰ تا ۴۰ نانومتر قرار داشت. **نتیجه‌گیری:** نانوذرات آهن با موفقیت بوسیله عصاره دانه شنبلیله سنتز شد. پارامترهای فیزیکی مانند مدت زمان واکنش، دمای آن و نسبت حجم مخلوط عصاره به محلول نمک آهن می‌توانند اندازه متوسط نانوذرات آهن را کنترل کنند.

مخففها: CCD، طراحی مرکب مرکزی؛ DPPH، ۲،۲- دی فنیل-۱- پیکریل هیدرازیل؛ FTIR، تبدیل فوریه طیف‌سنجی مادون قرمز؛ INPs، نانوذرات آهن؛ RSM، روش سطح پاسخ؛ SEM، میکروسکوپ الکترونی روبشی؛ TEM، میکروسکوپ الکترونی عبوری

* نویسنده مسؤول: hajiaghaee@imp.ac.ir

تاریخ دریافت: ۶ مهر ۱۴۰۰؛ **تاریخ دریافت اصلاحات:** ۹ دی ۱۴۰۰؛ **تاریخ پذیرش:** ۱۱ دی ۱۴۰۰

doi: 10.52547/jmp.21.81.22